

# A risk assessment model for the prognosis of osteosarcoma utilizing differentially expressed lncRNAs

KAI SUN and JIANMIN ZHAO

Department of Orthopedics, Affiliated Hospital of Inner Mongolia Medical University,  
Hohhot, Inner Mongolia Autonomous Region 010050, P.R. China

Received December 14, 2017; Accepted November 1, 2018

DOI: 10.3892/mmr.2018.9768

**Abstract.** The present study was conducted to establish a risk assessment model for evaluating osteosarcoma prognosis based on prognosis-associated long non-coding RNA (lncRNA) expression. Human osteosarcoma expression profiles were obtained from the NCBI GEO and EBI ArrayExpress databases and differentially expressed lncRNAs between good and poor prognosis groups were evaluated using Student's t-test and Wilcoxon rank test in R (v. 3.1.0). A multivariate Cox regression was used to establish a risk assessment system based on lncRNA expression levels, with the associated regression coefficients used as the weight. Survival analysis and receiver operating characteristic (ROC) curves were constructed to verify the accuracy of the risk assessment model. Associations between the prognosis, risk assessment model and clinical features were also investigated using univariate and multivariate Cox regression analyses. Furthermore, differentially expressed genes associated with the lncRNAs in the risk assessment model were identified, and functional enrichment analysis was performed. A total of 9 from the 211 differentially expressed lncRNAs were selected to establish the risk assessment model. The risk assessment model exhibited a good prognostic prediction ability, with high area under the curve values in the training and validation sets. Additionally, the calculated risk score based on the 9 selected lncRNAs was identified to be an independent prognostic factor for osteosarcoma. Furthermore, differentially expressed genes were primarily enriched in the cell cycle, oxidative phosphorylation and cell adhesion processes. The present study described a risk assessment model based on 9 significantly differentially expressed lncRNAs, which was identified to have a high accuracy in potentially predicting patient prognosis.

## Introduction

Osteosarcoma is one of the most common types of primary malignant bone cancer and is characterized by tumor cells directly forming osteoid tissue or immature bone (1-3). Epidemiological study has indicated a bimodal age distribution for osteosarcoma, with pubescent adolescents undergoing a rapid growth period at the greatest risk (4). While effective methods, including primary tumor excision, adjuvant radiotherapy and chemotherapy, have been widely adopted to improve osteosarcoma survival, the prognosis remains poor (5). The 5-year survival rate is >20% in high-risk patients treated with surgery alone (6), with an increase to a 30-40% survival rate when surgery is combined with adjuvant therapies, radiation or chemotherapy (7). Therefore, the identification of an effective prognostic factor able to optimize treatment and supply a novel therapeutic target to improve the clinical outcome for patients with osteosarcoma is required.

Long non-coding RNAs (lncRNAs) are >200 nucleotides and lack an open reading frame, and therefore are unable to be translated into a protein (8). With the expansion of gene research, lncRNAs have been identified to serve critical roles in a variety of cellular processes, including gene and protein regulation, transcription and post-transcription (9-11). The roles of lncRNAs in tumor-associated processes have also been widely examined, with certain lncRNAs having been demonstrated to be associated with histological grade in several tumor types (9). Furthermore, increasing evidence has suggested that lncRNAs may serve as useful prognostic biomarkers for certain tumors, including non-small cell lung cancer (12), metastatic breast cancer (13) and hepatocellular carcinomas (14). Previous studies have focused on the roles of lncRNAs in osteosarcoma prognosis: A specific lncRNA, taurine upregulated gene 1, was suggested to contribute to human osteosarcoma tumorigenesis by regulating POU domain class 2 transcription factor 1 expression (15). In addition, over-expression of the lncRNA BRAF-activated noncoding RNA was observed in osteosarcomas, with an increased expression associated with advanced clinical stage, distant metastasis and large tumor size (16). However, a reliable and effective risk assessment model for osteosarcoma prognosis is required.

In the present study, human osteosarcoma expression profiles were downloaded to screen prognosis-associated lncRNAs. Next, a risk assessment system was constructed

---

*Correspondence to:* Dr Jianmin Zhao, Department of Orthopedics, Affiliated Hospital of Inner Mongolia Medical University, 1 Tongdao Road, Hohhot, Inner Mongolia Autonomous Region 010050, P.R. China  
E-mail: duangsksk@163.com

**Key words:** osteosarcoma, long non-coding RNA, risk assessment model, prognosis

based on the expressions of prognosis-associated lncRNAs, with the associated regression coefficients used as the weight. Survival analysis for the risk assessment model was conducted using a training set and validation set. Concomitantly, the risk value of each sample was calculated based on the risk score equation. Independent osteosarcoma prognostic factors and correlations between risk score and clinical features were also examined. Additionally, differentially expressed genes associated with the lncRNAs in the risk assessment model were identified, and functional enrichment was performed. The present study aimed to identify a novel risk assessment model for osteosarcoma prognosis, and thereby aid in patient drug selections and adjustments.

## Materials and methods

**Data and grouping.** Human osteosarcoma-associated expression profiles were downloaded from the NCBI Gene Expression Omnibus (GEO, <https://www.ncbi.nlm.nih.gov/geo/>) and EBI ArrayExpress (<https://www.ebi.ac.uk/arrayexpress/>) databases. The expression data were included when meet the following criteria: i) The osteosarcoma sample data must contain clinical information and a survival prognosis; and ii) the annotation platform must contain lncRNA annotation information or provide complete sequence detection of the probe reporter. Ultimately, two data sets, GSE21257 (n=53) and GSE39055 (n=37), were identified and obtained using the GPL10295 human-6 v2.0 (using nuIDs as identifier; Illumina, Inc., San Diego, CA, USA) and GPL14951 HumanHT-12 WG-DASL v4.0 R2 expression beadchips (Illumina, Inc.), respectively. The GSE21257 set was selected as the training set, and the GSE39055 was set as the validation set. The clinical data for these two data sets are summarized in Table I. The lncRNAs in these two data sets were analyzed using Basic Local Alignment Search Tool and a human genome reference sequence (UCSC hg19; <http://hgdownload.soe.ucsc.edu/downloads.html>).

**Screening for significantly differentially expressed lncRNAs.** The 53 training set samples (GSE21257) were divided into a bad prognosis group (survival time <36 months; n=17) or good prognosis group (alive, survival time ≥60 months; n=21). The expression levels of lncRNAs between these two groups were then compared to identify significantly differentially expressed lncRNAs by using a Student's t-test or Wilcoxon rank test in R v3.1.0 with the thresholds of false discovery rate (FDR) <0.05 and log<sub>2</sub> fold change (FC) >0.263. lncRNAs revealed to be significantly differentially expressed using these two cut-offs were selected for two-way hierarchical clustering and subsequent analysis.

**Screening for prognosis-associated lncRNAs.** To screen prognosis-associated lncRNAs, significantly differentially expressed lncRNAs selected from the training set (53 osteosarcoma samples) were examined via Cox regression analysis (univariate and multivariate) in R v3.1.0 (<https://www.r-project.org/>) as described previously (17). P<0.05 obtained by log-rank test was set as the cut-off criterion.

**Establishing a risk assessment model.** To establish a risk assessment system, the obtained prognosis-associated lncRNAs were

evaluated using a multivariate Cox regression with the regression coefficients (β) used as the weight. The risk value for each sample was obtained using the following equation: Risk score =  $\beta_{\text{lncRNA1}} \times \text{expr}_{\text{lncRNA1}} + \beta_{\text{lncRNA2}} \times \text{expr}_{\text{lncRNA2}} + \dots + \beta_{\text{lncRNA}_n} \times \text{expr}_{\text{lncRNA}_n}$ . The survival risk of cancer in the validation set was assessed using the β-value acquired from the training set.

**Evaluating the risk assessment model.** The samples in the validation set were divided into high risk and low risk groups according to the median risk scores calculated in the risk assessment model. The median value was included in the low risk group. Kaplan-Meier survival curve analysis was used to estimate the overall survival (OS) rates for patients in the high risk and low risk groups, followed by a log-rank test (18), which was used to assess the survival differences between the high-risk and the low-risk groups. P<0.05 was considered to indicate a statistically significant difference. Furthermore, a ROC curve was used to evaluate the classification efficiency of the obtained risk assessment model. The expression distributions of the selected lncRNAs were also analyzed in the training and validation sets.

**Correlation between the risk assessment model and clinical features.** Associations between prognosis and clinical features, which include risk score, age, sex, grade and tumor metastasis, were evaluated using univariate and multivariate Cox regression analyses. Furthermore, hierarchical analysis was also performed using clinical features that were significantly associated with the risk score. Associations between the different risk groups and the survival prognosis were analyzed under the same clinical condition.

**Identifying prognosis-associated genes and functional enrichment analysis.** The genes regulated by the significantly differentially expressed lncRNA were obtained using MEM software (<http://biit.cs.ut.ee/mem/>) (19,20). Subsequently, the differentially expressed genes between high-risk group and low-risk group in the training set were identified with the thresholds of |log FC|>0.5 and FDR<0.05 using Limma (21,22). These differentially expressed were considered prognosis-associated genes.

In order to identify the biological processes and signaling pathways that involved these prognosis-associated genes, the Database for Annotation, Visualization and Integrated Discovery (<https://david.ncifcrf.gov/>) was used to perform Gene Ontology (<http://geneontology.org/>) analysis, and the Kyoto Encyclopedia of Genes and Genomes (KEGG; <https://www.genome.jp/kegg/>) database was utilized for enrichment analysis with the cut-off of P<0.05.

## Results

**Screened differentially expressed lncRNAs.** A total of 233 differentially expressed lncRNAs were identified using the Student's t-test (Fig. 1A) and 298 were identified using the Wilcoxon rank test (Fig. 1B). The 211 overlapping lncRNAs identified by Student's t-test and Wilcoxon rank test were selected for subsequent analysis (Fig. 1C). The two-way hierarchical clustering based on these 211 lncRNAs indicated significant differences between the bad and good prognosis groups (Fig. 1D).

Table I. Clinical information for training and validation sets.

Variable	GSE21257 (n=53)	GSE39055 (n=37)	P-value
Age (mean $\pm$ SD)	18.71 $\pm$ 12.19	13.47 $\pm$ 11.34	0.0402 <sup>a</sup>
Sex (male/female)	34/19	20/17	0.4572 <sup>b</sup>
Metastases (yes/no)	34/19	-	-
Death (dead/alive)	23/30	10/27	0.1728 <sup>b</sup>
Overall survival time (mean $\pm$ SD)	68.55 $\pm$ 59.34	52.92 $\pm$ 50.14	0.1813 <sup>a</sup>

SD, standard deviation; <sup>a</sup>Student's t-test; <sup>b</sup>Chi-square test.

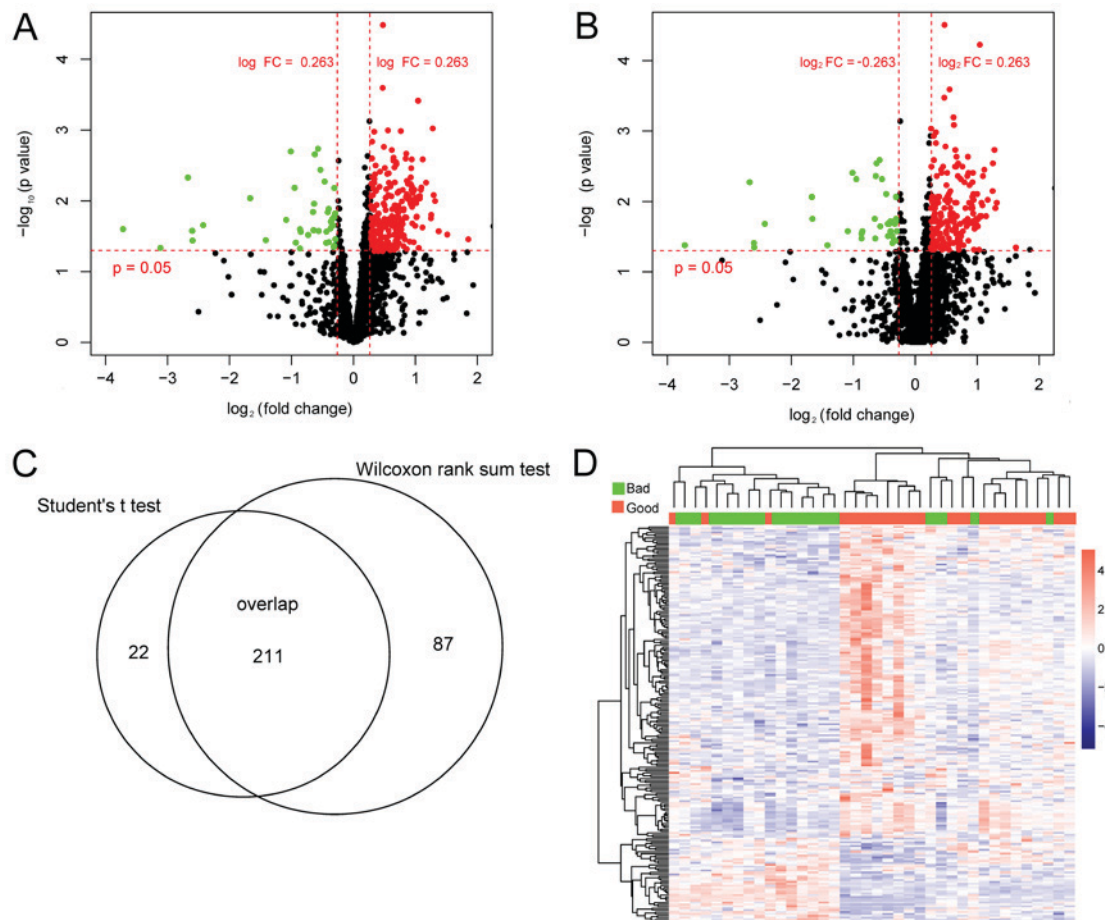


Figure 1. Significantly differentially expressed lncRNAs identified in the training set. Volcanic maps of differentially expressed lncRNAs identified via (A) Student's t-test or (B) Wilcoxon rank test. The abscissa indicates the  $\log_2$  FC and the ordinate indicates the negative logarithm of the P-value. Red nodes indicate upregulated lncRNA, green nodes represent downregulated lncRNA and black nodes represent non-differentially expressed lncRNA. (C) Overlapping differentially expressed lncRNAs between the Student's t-test and Wilcoxon rank test. (D) A two-way hierarchical clustering map based on the 211 differentially expressed lncRNAs. FC, fold change; lncRNA, long non-coding RNA.

**Construction of the lncRNA risk assessment model.** In the training set, 84 out of the 211 differentially expressed lncRNAs were identified to be associated with the survival prognosis ( $P < 0.05$ ). Next, 9 lncRNAs (CH17-360D5.2, LINC00987, LINC01526, RP11-15A1.3, RP11-213H15.1, RP11-218F4.1, RP11-242F11.2, RP11-411H5.1 and RP11-834C11.5) from the 84 prognosis-associated lncRNAs were additionally screened via a multiple Cox regression analysis ( $P < 0.05$ ; Table II). All samples in training set were divided into low expression group ( $\leq$  median value) and high expression group ( $>$  median value) based on

the expression levels of these 9 individual lncRNAs, separately. The Kaplan-Meier survival curve analysis revealed that the samples with low expression of RP11-411H5.1, RP11-834C11.5 or LINC00987 had significantly increased survival ratio (Fig. 2). Samples with increased expression of LINC01526, RP11-15A1.3, RP11-213H15.1, RP11-218F4.1, RP11-242F11.2 or CH17-360D5.2 exhibited markedly increased survival ratios (Fig. 2).

A risk assessment model was established based on these 9 lncRNAs according to the following formula: Risk score =  $(-2.0368) \times \text{Exp}_{\text{CH17-360D5.2}} + (-0.0683) \times \text{Exp}_{\text{LINC00987}} + (-6.0924)$

Table II. Information of 9 lncRNAs screened from the 53 osteosarcoma samples in GSE21257 to build the risk assessment model.

Long non-coding RNA	Coefficient	Hazard ratio	95% confidence interval	P-value
CH17-360D5.2	-2.037	0.112	0.042-0.301	0.005
LINC00987	-0.068	0.111	0.067-0.186	0.037
LINC01526	-6.092	0.160	0.023-0.213	0.016
RP11-15A1.3	-3.673	0.107	0.092-0.125	0.024
RP11-213H15.1	-4.925	0.163	0.035-0.752	0.034
RP11-218F4.1	-0.160	0.607	0.301-0.802	0.028
RP11-242F11.2	-3.758	0.781	0.296-0.964	0.013
RP11-411H5.1	-0.009	0.243	0.219-0.629	0.028
RP11-834C11.5	7.861	3.510	1.090-4.113	0.016

lncRNA, long non-coding RNA.

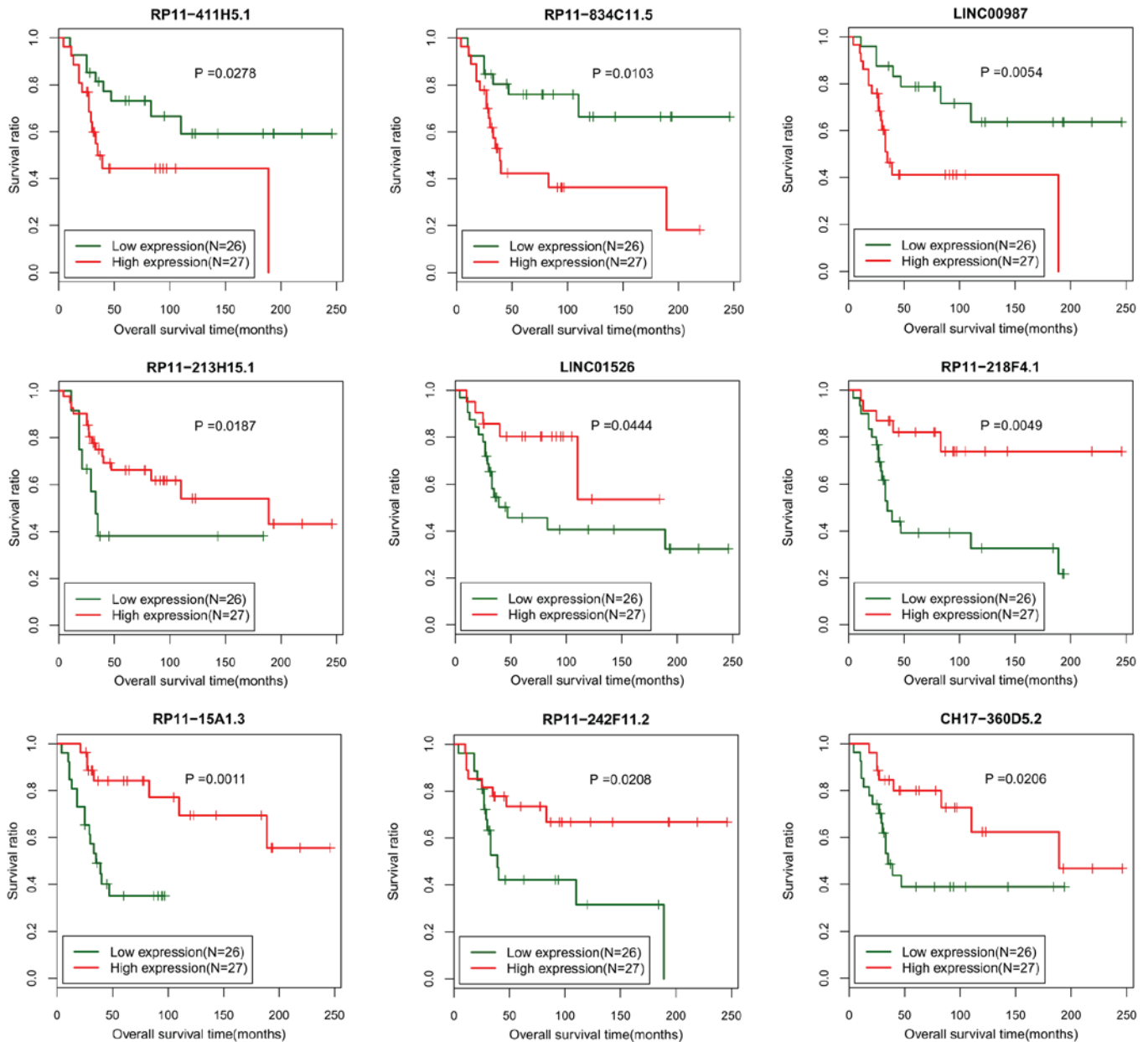


Figure 2. Kaplan-Meier curves of overall survival for the 9 long non-coding RNAs in the risk assessment model. The red lines indicate samples with high expression levels and green lines indicate samples with low expression levels.



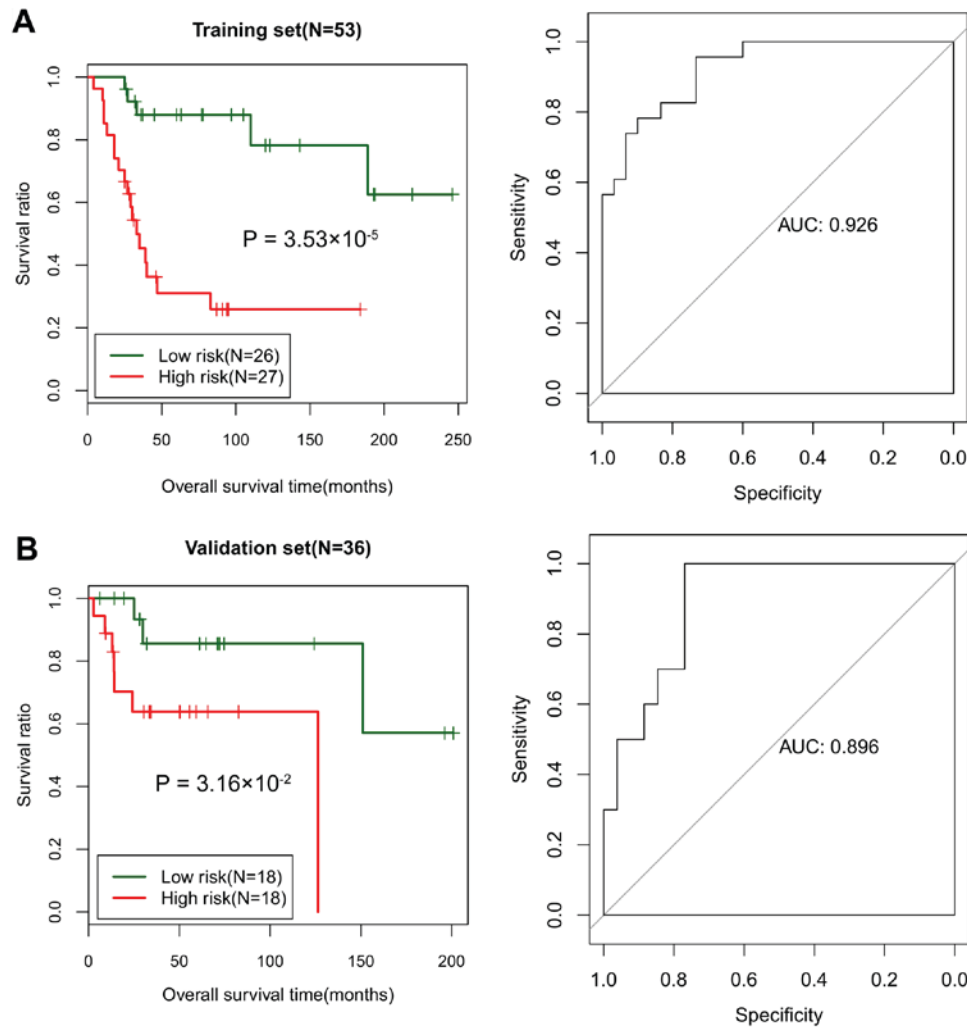


Figure 3. ROC curve assessing high-risk and low-risk patients based on the risk assessment model. ROC curves for the (A) training set and (B) validation set, with the abscissa indicating the sensitivity and the ordinate indicating the specificity. ROC, receiver operating characteristic; AUC, area under the ROC curve.

$$\begin{aligned} & \text{xExp}_{\text{LINC01526}} + (-3.6727) \text{xExp}_{\text{RP11-15A1.3}} + (-4.9249) \text{xExp}_{\text{RP11-213H15.1}} \\ & + (-0.1602) \text{xExp}_{\text{RP11-218F4.1}} + (-3.7582) \text{xExp}_{\text{RP11-242F11.2}} + (-0.0093) \\ & \text{xExp}_{\text{RP11-411H5.1}} + (7.8606) \text{xExp}_{\text{RP11-834C11.5}}. \end{aligned}$$

**Verification of the lncRNA risk assessment model.** All samples in the training set were divided into high-risk (n=26) and low-risk (n=27) groups based on the median risk score. The log-rank test indicated that the survival ratio of the high-risk group was significantly increased compared with that of the low-risk group ( $P=3.532 \times 10^{-5}$ ; Fig. 3A). The area under the curve (AUC) was 0.926, suggesting a good prognosis prediction ability of the risk assessment system (Fig. 3A).

In the validation set, the samples were divided into high-risk (n=18) and low-risk (n=18) groups based on the median risk score. The log-rank test also indicated a markedly increased survival ratio of the high-risk group compared with the low-risk group ( $P=0.032$ ; Fig. 3B). The AUC for the ROC curve based on the risk assessment system was 0.896 (Fig. 3B). In the validation set, the RP11-411H5.1, RP11-834C11.5 and LINC00987 were significantly upregulated in the samples belonging to the high-risk group ( $P<0.005$ ; Fig. 4). The other 6 lncRNAs (LINC01526, RP11-15A1.3, RP11-213H15.1, RP11-218F4.1, RP11-242F11.2 and CH17-360D5.2) were

significantly downregulated in the samples belonging to the high-risk group ( $P<0.05$ ; Fig. 4).

**Risk score is an independent prognostic factor for osteosarcoma.** Univariate and multivariate Cox regression analyses were conducted to investigate potential associations between the independent prognostic factors and prognosis. In the training set, risk score [ $P=3.530 \times 10^{-5}$ ; 95% confidence interval (CI), 2.492-13.030]; age ( $P=0.038$ ; 95% CI, 0.134-0.985), grade ( $P=0.011$ ; 95% CI, 1.284-1.867) and tumor metastasis ( $P=2.380 \times 10^{-7}$ ; 95% CI, 1.963-3.649) were identified to be significantly associated with the prognosis according to the univariate Cox regression analysis. In addition, the multivariate Cox regression analysis demonstrated that risk score ( $P=0.028$ ; 95% CI, 1.563-5.785), grade ( $P=0.01$ ; 95% CI, 1.291-1.872) and tumor metastasis ( $P<0.001$ ; 95% CI, 1.694-5.312) were identified as independent prognostic factors for osteosarcoma (Table III). The effect of risk score on prognosis was then analyzed using a hierarchical analysis, and it was indicated that patients without tumor metastasis in the low-risk group ( $P=1.249 \times 10^{-3}$ ) and high-risk group ( $P=0.005$ ) exhibited significantly improved prognoses (Fig. 5).

Table III. Univariate and multivariate Cox regression analysis for independent prognostic factors of osteosarcoma according to the 53 osteosarcoma samples in the GSE21257 data set.

Variables	Univariate analysis			Multivariate analysis		
	HR	95% CI	P-value	HR	95% CI	P-value
Risk score (high/low)	7.574	2.492-13.030	$3.53 \times 10^{-5}$	1.868	1.563-5.785	0.028
Age (<18/≥18)	0.363	0.134-0.985	0.038	0.738	0.228-2.386	0.814
Sex (male/female)	1.403	0.588-3.348	0.444	-	-	-
Grade (G1+G2/G3+G4)	1.496	1.284-1.867	0.011	1.504	1.291-1.872	0.014
Tumor metastases (yes/no)	2.218	1.963-3.649	$2.38 \times 10^{-7}$	1.211	1.037-2.759	$2.71 \times 10^{-3}$

HR, hazard ratio; CI, confidence interval.

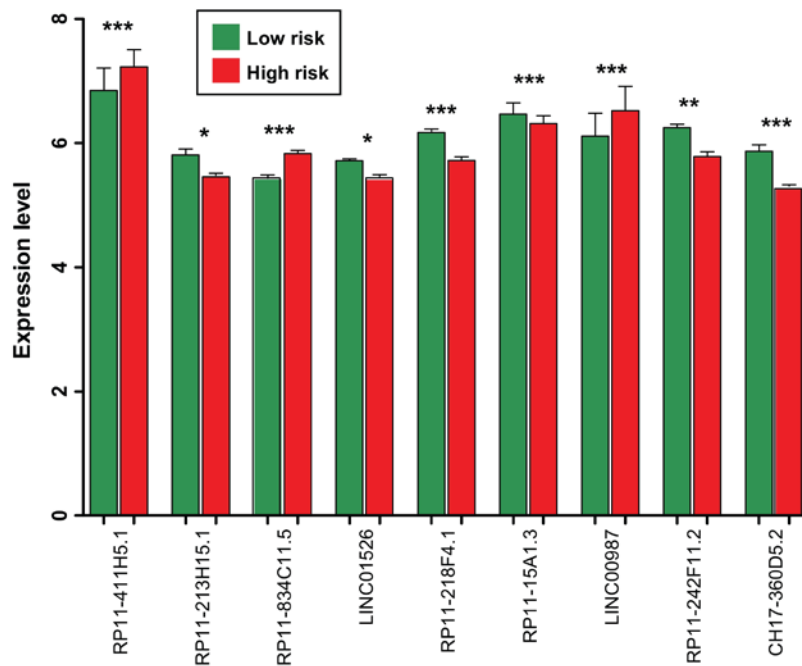


Figure 4. Expression levels for the 9 selected long non-coding RNAs in the validation set. \* $P < 0.05$ , \*\* $P < 0.01$  and \*\*\* $P < 0.005$ .

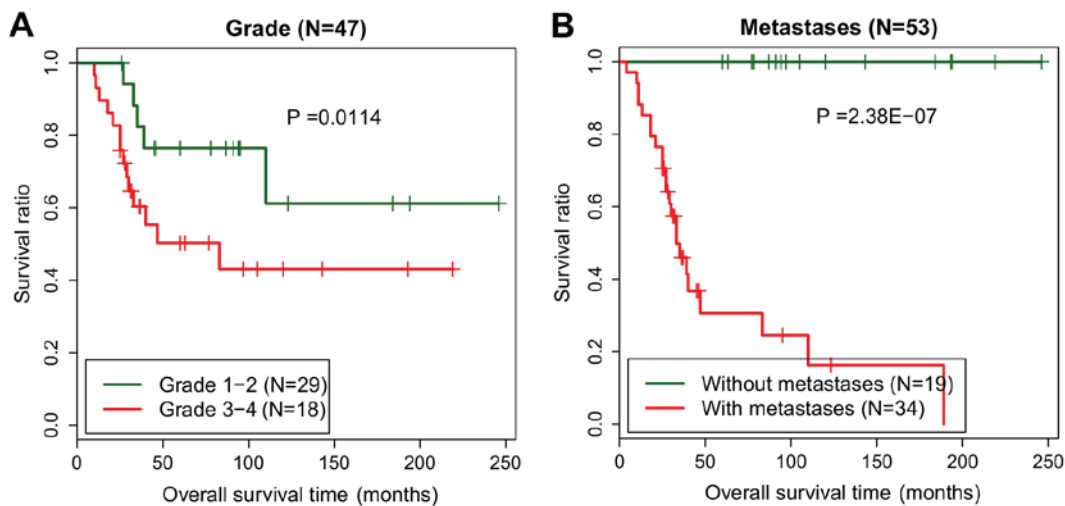


Figure 5. Kaplan-Meier curves of overall survival between high-risk and low-risk patients in the training set based on the hierarchical analysis. Kaplan-Meier curves for (A) samples with grade I-II (green line) and samples with grade III-IV (red line) tumors and for (B) samples without tumor metastasis (green line) and samples with tumor metastasis (red line).

Table IV. Top 10 upregulated and downregulated differentially expressed genes associated with the 9 lncRNAs in the risk assessment model.

A, Upregulated genes

	Log FC	P-value	FDR
RPLP1	1.331	$1.860 \times 10^{-6}$	$1.305 \times 10^{-4}$
UQCRH	1.298	$7.820 \times 10^{-7}$	$5.480 \times 10^{-5}$
PTMA	1.293	$6.750 \times 10^{-6}$	$4.734 \times 10^{-4}$
RPL23	1.237	$4.850 \times 10^{-6}$	$3.399 \times 10^{-4}$
SUMO2	1.209	$6.110 \times 10^{-6}$	$4.281 \times 10^{-4}$
PTGES3	1.165	$6.770 \times 10^{-6}$	$4.743 \times 10^{-4}$
NDUFB9	1.133	$1.110 \times 10^{-6}$	$7.790 \times 10^{-5}$
RPL27A	1.131	$1.520 \times 10^{-6}$	$1.068 \times 10^{-4}$
KPNA2	1.108	$3.180 \times 10^{-6}$	$2.228 \times 10^{-4}$
ACTR3	1.061	$4.780 \times 10^{-6}$	$3.348 \times 10^{-4}$

B, Downregulated genes

	Log FC	P-value	FDR
C1S	-0.501	$6.443 \times 10^{-4}$	$4.517 \times 10^{-2}$
IFI44L	-0.503	$4.218 \times 10^{-4}$	$2.957 \times 10^{-2}$
FAP	-0.506	$4.576 \times 10^{-4}$	$3.208 \times 10^{-2}$
CYP27A1	-0.513	$4.440 \times 10^{-6}$	$3.110 \times 10^{-4}$
CD163	-0.526	$1.821 \times 10^{-4}$	$1.277 \times 10^{-2}$
ETV5	-0.526	$3.940 \times 10^{-6}$	$2.759 \times 10^{-4}$
SDC1	-0.528	$1.390 \times 10^{-5}$	$9.719 \times 10^{-4}$
HLA-DMA	-0.535	$3.650 \times 10^{-5}$	$2.559 \times 10^{-3}$
CCL8	-0.537	$4.822 \times 10^{-4}$	$3.380 \times 10^{-2}$
MOXD1	-0.574	$5.927 \times 10^{-4}$	$4.155 \times 10^{-2}$

FC, fold change; FDR, false discovery rate.

**Functional enrichment of prognosis-associated genes.** A total of 250 differentially expressed genes, including 232 upregulated and 18 downregulated, were identified among the genes that were associated with the 9 lncRNAs identified using the risk assessment model. The top 10s upregulated [ribosomal protein lateral stalk subunit P1 (*RPLP1*), ubiquinol-cytochrome c reductase hinge protein (*UQCRH*), prothymosin alpha (*PTMA*), ribosomal protein L23 (*RPL23*), small ubiquitin-like modifier 2, prostaglandin E synthase 3, NADH:ubiquinone oxidoreductase subunit B9 (*NDUFB9*), ribosomal protein L27a (*RPL27A*), karyopherin subunit alpha 2 (*KPNA2*) and ARP3 actin related protein 3 homolog] and downregulated [complement C1s (*C1S*), interferon induced protein 44 like, fibroblast activation protein alpha, cytochrome P450 family 27 subfamily A member 1 (*CYP27A1*), CD163 molecule (*CD163*), ETS variant 5, syndecan 1 (*SDC1*), major histocompatibility complex, class II, DM alpha (*HLA-DMA*), C-C motif chemokine ligand 8 (*CCL8*) and monooxygenase DBH like 1] differentially expressed genes are listed in Table IV.

Furthermore, biological processes and signaling pathways were enriched for these 250 prognosis-associated genes.

For the biological process (BP) terms, genes were primarily enriched in the translation (including *RPLP1*, *RPL23* and *RPL27A*;  $P=2.080 \times 10^{-4}$ ), protein transport (including *RPL23* and *HLA-DMA*;  $P=7.654 \times 10^{-3}$ ), inflammatory response (including *C1S* and *CD163*;  $P=1.26 \times 10^{-2}$ ), oxidation reduction (including *UQCRH*, *NDUFB9* and *CYP27A1*;  $P=2.148 \times 10^{-2}$ ). KEGG pathway enrichment analysis suggested that these genes were primarily enriched in Ribosome (including *RPLP1*, *RPL23* and *RPL27A*;  $P=6.270 \times 10^{-7}$ ), Oxidative phosphorylation (including *UQCRH* and *NDUFB9*;  $P=1.355 \times 10^{-3}$ ), Glycolysis/Gluconeogenesis [lactate dehydrogenase B (*LDHB*), phosphoglycerate mutase family member 4 (*PGAM4*), aldolase, fructose-biphosphate C (*ALDOC*), dihydrolipoamide dehydrogenase (*DLD*) and dihydrolipoamide S-acetyltransferase (*DLAT*);  $P=2.965 \times 10^{-3}$ ) and Cell adhesion molecules (CAMs) (including *SDC1* and *HLA-DMA*;  $P=4.839 \times 10^{-2}$ ). The functional and pathway enrichment analyses indicated that TTK protein kinase (*TTK*), cyclin B1 (*CCNB1*) and BUB1 mitotic checkpoint serine/threonine kinase (*BUB1*) were markedly implicated in the cell cycle (Table V).

## Discussion

A total of 211 differentially expressed lncRNAs were identified, and 9 of them (CH17-360D5.2, LINC00987, LINC01526, RP11-15A1.3, RP11-213H15.1, RP11-218F4.1, RP11-242F11.2, RP11-411H5.1 and RP11-834C11.5) were selected to establish a risk assessment model for evaluating the prognosis of patients with osteosarcoma. In the training and validation sets selected, samples with low expression of RP11-411H5.1, RP11-834C11.5 or LINC00987 exhibited significantly increased survival ratios, and samples with increased expression levels of LINC01526, RP11-15A1.3, RP11-213H15.1, RP11-218F4.1, RP11-242F11.2 or CH17-360D5.2 exhibited significantly higher survival ratios.

The ROC curves revealed that this risk assessment model may serve as a good prognostic prediction system in the training (AUC=0.926) and validation sets (AUC 0.896). Furthermore, the risk score calculated based on the expression levels of these 9 lncRNAs was revealed to be an independent prognostic factor for osteosarcoma. Additionally, 250 differentially expressed genes associated with the 9 lncRNAs in the risk assessment model were identified. Functional enrichment analysis for these differentially expressed genes revealed that *UQCRH* and *NDUFB9* were significantly associated with oxidation reduction and oxidative phosphorylation. The gene product of *UQCRH* is a subunit of the respiratory chain protein ubiquinol cytochrome c reductase. *NDUFB9* (22 kDa) is an accessory subunit of the mitochondrial complex I NADH dehydrogenase in the membrane respiratory chain (23). Mutations in mitochondrial DNA or nuclear genes encoding mitochondrial proteins may lead to mitochondrial dysfunctions, which are essential for the respiratory chain/oxidative phosphorylation system (24). It has been suggested that aberrations in mitochondrial complex I NADH dehydrogenase activity may markedly promote breast cancer progression (25). Normal differentiated cells primarily use mitochondrial oxidative phosphorylation to generate energy for cellular processes, whereas cancer cells rely on aerobic glycolysis to generate energy for enhanced growth (26,27). In the present study, the pathway enrichment analysis revealed that *LDHB*,

Table V. Significantly enriched functions and pathways for the identified prognosis-associated genes.

Category	Term	Count	P-value	Genes
BP	GO:0006414; translational elongation	11	3.690x10 <sup>-6</sup>	RPS28, RPL23, RPL14, RPL7, RPS3A, RPLP1, RPS15, RPL27A, RPL23A, RPL7A, RPL10A
BP	GO:0006412; translation	16	2.080x10 <sup>-4</sup>	MRPL51, CARS, RPL14, NARS, RPL27A, RPL23A, RPS28, RPL7, RPL23, RPS3A, EIF1AX, RPS15, RPLP1, MRPL19, RPL10A, RPL7A
BP	GO:0006091; generation of precursor metabolites and energy	14	1.223x10 <sup>-3</sup>	UQCRC2, TXNL1, LDHB, NDUFB10, ALDOC, NDUFB9, DLAT, SLC25A13, UQCRH, PGAM4, SDHD, DLD, UQCRB, FH
BP	GO:0008283; cell proliferation	16	3.357x10 <sup>-3</sup>	MORF4L1, COPS2, STIL, PDPN, VTI1B, IFI16, RBBP7, GAS6, LGR4, SBDS, GOLPH3, PCNA, CKS2, BUB1, RAPIB, ASPM
BP	GO:0070271; protein complex biogenesis	17	5.484x10 <sup>-3</sup>	TCPI1, MSTO1, ALDOC, CAPZAI, GJAI, ANLN, CDH2, CENPJ, HLA-DMA, PICALM, UQCRH, GOPC, NPM1, PDGFC, ANGPT1, KPNA3, KPNB1
BP	GO:0006461; protein complex assembly	17	5.484x10 <sup>-3</sup>	TCPI1, MSTO1, ALDOC, CAPZAI, GJAI, ANLN, CDH2, CENPJ, HLA-DMA, PICALM, UQCRH, GOPC, NPM1, PDGFC, ANGPT1, KPNA3, KPNB1
BP	GO:0015031; protein transport	22	7.654x10 <sup>-3</sup>	GD12, GOLT1B, VTI1B, PPT1, CLTC, HLA-DMA, TIMM8B, RAB33B, NXT2, YWHAG, RPL23, RAB18, GOPC, NPM1, PCNA, YIPF5, KPNA3, KPNA2, SARIA, SEC24D, KPNB1, NMD3
BP	GO:0045184; establishment of protein localization	22	8.450x10 <sup>-3</sup>	GD12, GOLT1B, VTI1B, PPT1, CLTC, HLA-DMA, TIMM8B, RAB33B, NXT2, YWHAG, RPL23, RAB18, GOPC, NPM1, PCNA, YIPF5, KPNA3, KPNA2, SARIA, SEC24D, KPNB1, NMD3
BP	GO:0009611; response to wounding	17	8.564x10 <sup>-3</sup>	A2M, NMI, PDPN, CCL8, CIS, CD163, CCNB1, HDAC4, PLSCR1, CD55, SDC1, STAB1, MTPN, SERPINE1, VSIG4, CD14, NFXI
BP	GO:0006954; inflammatory response	12	1.264x10 <sup>-2</sup>	HDAC4, A2M, CD55, NMI, PDPN, STAB1, CCL8, CIS, VSIG4, CD14, CD163, NFXI
BP	GO:0065003; macromolecular complex assembly	19	1.558x10 <sup>-2</sup>	TCPI1, MSTO1, ALDOC, CAPZAI, GJAI, ANLN, CDH2, CENPJ, HLA-DMA, SMNDC1, PICALM, UQCRH, GOPC, RPS15, NPM1, PDGFC, ANGPT1, KPNA3, KPNB1
BP	GO:0007049; cell cycle	21	1.796x10 <sup>-2</sup>	PDPN, GMNN, TTK, ANLN, RBM7, CDC5L, UBE2C, CENPJ, MLF1, CCNB1, SBDS, GADD45GIP1, PSMA6, FANCD2, NPM1, CKS2, BUB1, KPNA2, MCTSI, ASPM, CDCA3
BP	GO:0055114; oxidation reduction	18	2.148x10 <sup>-2</sup>	UQCRC2, TXNL1, LDHB, NDUFB10, CYP51A1, NDUFB9, UGDH, MOXD1, MTRR, FDFIT1, MTHFD2, SLC25A13, CYP27A1, P4HA1, UQCRH, DLD, SDHD, UQCRB



Table V. Continued.

Category	Term	Count	P-value	Genes
BP	GO:0043933; macromolecular complex subunit organization	19	2.790x10 <sup>-2</sup>	<i>TCPI1, MSTO1, ALDOC, CAPZA1, GJA1, ANLN, CDH2, CENPJ, HLA-DMA, SMNDC1, PICALM, UQCRH, GOPC, RPS15, NPM1, PDGFC, ANGPT1, KPNA3, KPNB1</i>
BP	GO:0022402; cell cycle process	16	3.030x10 <sup>-2</sup>	<i>TTK, ANLN, RBM7, UBE2C, CENPJ, MLF1, CCNB1, SBDS, PSMA6, FANCD2, NPM1, CKS2, BUB1, KPNA2, ASPM, CDCA3</i>
BP	GO:0006886; intracellular protein transport	12	3.190x10 <sup>-2</sup>	<i>YWHAG, RPL23, NPM1, PCNA, VTIIB, CLTC, KPNA3, KPNA2, SARIA, KPNB1, SEC24D, TIMM8B</i>
BP	GO:0000279; M phase	11	3.283x10 <sup>-2</sup>	<i>CCNB1, FANCD2, BUB1, CKS2, TTK, RBM7, ANLN, UBE2C, KPNA2, ASPM, CDCA3</i>
BP	GO:0008104; protein localization	22	3.337x10 <sup>-2</sup>	<i>GDI2, GOLT1B, VTIIB, PPT1, CLTC, HLA-DMA, TIMM8B, RAB33B, NXT2, YWHAG, RPL23, RAB18, GOPC, NPM1, PCNA, YIPF5, KPNA3, KPNA2, SARIA, SEC24D, KPNB1, NMD3</i>
BP	GO:0010605; negative regulation of macromolecule metabolic process	19	3.693x10 <sup>-2</sup>	<i>IBTK, COPS2, BTAF1, A2M, MTDH, GMNN, FZD1, HAT1, RBBP7, UBE2C, HDAC4, SAP30, HDAC2, PSMA6, HEY1, PRKRA, NPM1, DNAJC1, NFX1</i>
PATHWAY	hsa03010; ribosome	11	6.270x10 <sup>-7</sup>	<i>RPS28, RPL23, RPL14, RPL7, RPS3A, RPLP1, RPS15, RPL27A, RPL23A, RPL7A, RPL10A</i>
PATHWAY	hsa00190; oxidative phosphorylation	8	1.355x10 <sup>-3</sup>	<i>UQCRC2, NDUFB10, UQCRH, NDUFB9, SDHD, COX7B, PPA2, UQCRB</i>
PATHWAY	hsa04260; cardiac muscle contraction	6	1.810x10 <sup>-3</sup>	<i>UQCRC2, ATP1B3, UQCRH, TNNC1, COX7B, UQCRB</i>
PATHWAY	hsa00010; glycolysis/Gluconeogenesis	5	2.965x10 <sup>-3</sup>	<i>LDHB, PGAM4, ALDOC, DLD, DLAT</i>
PATHWAY	hsa04110; cell cycle	7	3.570x10 <sup>-3</sup>	<i>CCNB1, YWHAG, HDAC2, BUB1, PCNA, TTK, RBX1</i>
PATHWAY	hsa04610; complement andcoagulation cascades	4	1.536x10 <sup>-2</sup>	<i>A2M, CD55, SERPINE1, C1S</i>
PATHWAY	hsa04142; lysosome	4	4.059x10 <sup>-2</sup>	<i>CTSO, PPT1, CD164, CLTC</i>
PATHWAY	hsa03040; spliceosome	4	4.532x10 <sup>-2</sup>	<i>HSPA1A, CDC5L, PRPF18, SMNDC1</i>
PATHWAY	hsa04514; cell adhesion molecules	4	4.839x10 <sup>-2</sup>	<i>ALCAM, SDC1, CDH2, HLA-DMA</i>

BP, biological process.

*PGAM4*, *ALDOC*, *DLD* and *DLAT* were involved in the glycolysis/gluconeogenesis pathway. Therefore, the lncRNAs in the risk assessment model may target the *UQCRH* and *NDUFB9* to regulate the oxidation reduction, oxidative phosphorylation and glycolysis/gluconeogenesis which are important for the improved growth of osteosarcoma cells.

The functional and pathway enrichment analyses indicated that *TTK*, *CCNB1* and *BUB1* were markedly implicated in the cell cycle. Huang *et al* (28) demonstrated that *FKBP14* overexpression may promote osteosarcoma carcinogenesis and be associated with poor prognosis. Threonine and tyrosine protein kinase (TTK), also known as the human monopolar spindle 1, is a dual serine/ threonine and tyrosine protein kinase (29). It has been revealed that the suppressed TTK expression identified in osteosarcoma cell lines may significantly decrease the cell proliferation and migration (30). In the study of Huang *et al* (28), *FKBP14* knockdown markedly decreased cell cycle associated CCNB1 protein expression. An additional study indicated that the abundance of CCNB1 mRNA and protein is increased normally from G1 to G2 phase (31). Budding uninhibited by benzimidazoles 1, the product of *BUB1*, is required for accurate chromosome segregation during mitosis. Upregulation and hyper-phosphorylation of *BUB1* may promote malignant transformation in SV40 Tag-induced transgenic mouse models (32). Therefore, the lncRNAs in the risk assessment model may promote progression of osteosarcoma by targeting *TTK*, *CCNB1* and *BUB1* to affect cell cycle.

In patients with cancer, complex signaling pathways affect survival and prognosis, with metastasis being the major cause of morbidity and mortality and accounting for ~90% of cancer mortalities (33). Metastasis includes an essential step of adhesion and it is affected by the surrounding extracellular matrix (ECM) (34). Focal adhesion is a prerequisite for cellular motility, which is essential to cancer metastasis, and is also involved in the settling of metastatic cancer cells at a distal site (35). Focal adhesion is commonly achieved by connecting the cellular cytoskeleton with ECM components or by connecting adjoining intracellular cytoskeletons (34). Focal adhesion expression has been suggested to be associated with cell migration and normally indicates a poor prognosis (36). Focal adhesion and the ECM have been commonly associated in osteosarcomas, with these factors investigated as potential antitumor targets (37,38). In the present study, 4 differentially expressed genes (*ALCAM*, *SDCI*, *CDH2* and *HLA-DMA*) associated with the 9 lncRNAs in the risk assessment model were significantly involved in CAMs. Therefore, the lncRNAs in the risk assessment model may have important roles in the progression of osteosarcoma by targeting *ALCAM*, *SDCI*, *CDH2* and *HLA-DMA* to regulate the cell adhesion molecules.

In the present study, a risk assessment model was established based on 9 differently expressed lncRNAs and exhibited the potential to be used for assessing prognosis in patients with osteosarcoma. The differentially expressed genes associated with the 9 lncRNAs in this risk assessment model were identified to be associated with oxidation reduction, oxidative phosphorylation, glycolysis/gluconeogenesis, cell cycle and cell adhesion molecules. The results presented in the present study may provide additional insight into the mechanisms of osteosarcoma tumorigenesis. However, certain limitations in the present study remain, including sample size. In addition,

the 9 identified potential prognostic lncRNAs require additional experimental validation to fully assess their predictive prognosis abilities in an independent cohort of patients with osteosarcoma.

## Acknowledgements

Not applicable.

## Funding

No funding was received.

## Availability of data and materials

The datasets analyzed during the current study are available in the Gene Expression Omnibus repository (accession nos. GSE21257 and GSE39055).

## Authors' contributions

KS and JZ analyzed and interpreted the gene expression data and wrote the manuscript. Both authors read and approved the final manuscript

## Ethics approval and consent to participate

Not applicable.

## Patient consent for publication

Not applicable.

## Competing interests

The authors declare that they have no competing interests

## References

1. Duchman KR, Gao Y and Miller BJ: Prognostic factors for survival in patients with high-grade osteosarcoma using the Surveillance, Epidemiology, and End Results (SEER) program database. *Cancer Epidemiol* 39: 593-599, 2015.
2. Mirabello L, Troisi RJ and Savage SA: Osteosarcoma incidence and survival rates from 1973 to 2004: Data from the surveillance, epidemiology, and end results Program. *Cancer* 115: 1531-1543, 2009.
3. Wang W, Li X, Meng FB, Wang ZX, Zhao RT and Yang CY: Effects of the long non-coding RNA HOST2 on the proliferation, migration, invasion and apoptosis of human osteosarcoma cells. *Cellular Physiol Biochem* 43: 320-330, 2017.
4. Whelan J, McTiernan A, Cooper N, Wong YK, Francis M, Vernon S and Strauss SJ: Incidence and survival of malignant bone sarcomas in England 1979-2007. *Int J Cancer* 131: E508-E517, 2012.
5. Ottaviani G and Jaffe N: The epidemiology of osteosarcoma. *Cancer Treat Res* 152: 3-13, 2009.
6. Fellenberg J, Bernd L, Delling G, Witte D and Zahlten-Hinguranage A: Prognostic significance of drug-regulated genes in high-grade osteosarcoma. *Mod Pathol* 20: 1085-1094, 2007.
7. Allison DC, Carney SC, Ahlmann ER, Hendifar A, Chawla S, Fedenko A, Angeles C and Menendez LR: A meta-analysis of osteosarcoma outcomes in the modern medical era. *Sarcoma* 2012: 704872, 2012.
8. Jandura A and Krause HM: The new RNA world: Growing evidence for long noncoding RNA functionality. *Trends Genet* 33: 665-675, 2017.

9. Li X, Wu Z, Fu X and Han W: Long noncoding RNAs: Insights from biological features and functions to diseases. *Med Res Rev* 33: 517-553, 2013.
10. Guttman M and Rinn JL: Modular regulatory principles of large non-coding RNAs. *Nature* 482: 339-346, 2012.
11. Cheetham SW, Gruhl F, Mattick JS and Dinger ME: Long noncoding RNAs and the genetics of cancer. *Br J Cancer* 108: 2419-2425, 2013.
12. Ji P, Diederichs S, Wang W, Böing S, Metzger R, Schneider PM, Tidow N, Brandt B, Buerger H, Bulk E, *et al*: MALAT-1, a novel noncoding RNA, and thymosin beta4 predict metastasis and survival in early-stage non-small cell lung cancer. *Oncogene* 22: 8031-8041, 2003.
13. Gupta RA, Shah N, Wang KC, Kim J, Horlings HM, Wong DJ, Tsai MC, Hung T, Argani P, Rinn JL, *et al*: Long non-coding RNA HOTAIR reprograms chromatin state to promote cancer metastasis. *Nature* 464: 1071-1076, 2010.
14. Yang Z, Zhou L, Wu LM, Lai MC, Xie HY, Zhang F and Zheng SS: Overexpression of long non-coding RNA HOTAIR predicts tumor recurrence in hepatocellular carcinoma patients following liver transplantation. *Ann Surg Oncol* 18: 1243-1250, 2011.
15. Xie CH, Cao YM, Huang Y, Shi QW, Guo JH, Fan ZW, Li JG, Chen BW and Wu BY: Long non-coding RNA TUG1 contributes to tumorigenesis of human osteosarcoma by sponging miR-9-5p and regulating POU2F1 expression. *Tumour Biol* 37: 15031-15041, 2016.
16. Peng ZQ, Lu RB, Xiao DM and Xiao ZM: Increased expression of the lncRNA BANCER and its prognostic significance in human osteosarcoma. *Genet Mol Res* 15: 2016.
17. Wang P, Wang Y, Hang B, Zou X and Mao JH: A novel gene expression-based prognostic scoring system to predict survival in gastric cancer. *Oncotarget* 7: 55343-55351, 2016.
18. Bland JM and Altman DG: The logrank test. *BMJ* 328: 1073, 2004.
19. Adler P, Kolde R, Kull M, Tkachenko A, Peterson H, Reimand J and Vilo J: Mining for coexpression across hundreds of datasets using novel rank aggregation and visualization methods. *Genome Biol* 10: R139, 2009.
20. Kolde R, Laur S, Adler P and Vilo J: Robust rank aggregation for gene list integration and meta-analysis. *Bioinformatics* 28: 573-580, 2012.
21. Ritchie ME, Phipson B, Wu D, Hu Y, Law CW, Shi W and Smyth GK: Limma powers differential expression analyses for RNA-sequencing and microarray studies. *Nucleic Acids Res* 43: e47, 2015.
22. Phipson B, Lee S, Majewski IJ, Alexander WS and Smyth GK: Robust hyperparameter estimation protects against hypervariable genes and improves power to detect differential expression. *Ann Appl Stat* 10: 946-963, 2016.
23. Lin X, Wells DE, Kimberling WJ and Kumar S: Human NDUFB9 gene: Genomic organization and a possible candidate gene associated with deafness disorder mapped to chromosome 8q13. *Hum Hered* 49: 75-80, 1999.
24. Ishikawa K, Takenaga K, Akimoto M, Koshikawa N, Yamaguchi A, Imanishi H, Nakada K, Honma Y and Hayashi J: ROS-generating mitochondrial DNA mutations can regulate tumor cell metastasis. *Science* 320: 661-664, 2008.
25. Santidrian AF, Matsunoyagi A, Ritland M, Seo BB, LeBoeuf SE, Gay LJ, Yagi T and Felding-Habermann B: Mitochondrial complex I activity and NAD<sup>+</sup>/NADH balance regulate breast cancer progression. *J Clin Invest* 123: 1068-1081, 2013.
26. Burk D and Schade AL: On respiratory impairment in cancer cells. *Science* 124: 267-272, 1956.
27. Heiden MG and Thompson CB: Understanding the warburg effect: The metabolic requirements of cell proliferation. *Science* 324: 1029-1033, 2009.
28. Huang Z, Li J, Du S, Tang Y, Huang L, Xiao L and Tong P: FKBP14 overexpression contributes to osteosarcoma carcinogenesis and indicates poor survival outcome. *Oncotarget* 7: 39872-39884, 2016.
29. Liu X, Liao W, Yuan Q, Ou Y and Huang J: TTK activates Akt and promotes proliferation and migration of hepatocellular carcinoma cells. *Oncotarget* 6: 34309-34320, 2015.
30. Dong Z, Sun K, Luan Y, Chen Y, Wang W, Liu D, Cheng C, Xiong F and Xi Y: Expression and clinical significance of threonine and tyrosine protein kinase (TTK) in osteosarcoma. *Translational Cancer Res* 6: 285-292, 2017.
31. Gentric G, Maillet V, Paradis V, Couton D, L'Hermitte A, Panasyuk G, Fromenty B, Celton-Morizur S and Desdouets C: Oxidative stress promotes pathologic polyploidization in nonalcoholic fatty liver disease. *J Clin Invest* 125: 981-992, 2015.
32. Guo C, Wu G, Chin JL, Bauman G, Moussa M, Wang F, Greenberg NM, Taylor SS and Xuan JW: Bub1 up-regulation and hyperphosphorylation promote malignant transformation in SV40 Tag-Induced transgenic mouse models. *Cancer Res* 66: 713, 2006.
33. Seyfried TN and Huysentruyt LC: On the origin of cancer metastasis. *Crit Rev Oncog* 18: 43-73, 2013.
34. Guan X: Cancer metastases: Challenges and opportunities. *Acta Pharm Sin B* 5: 402-418, 2015.
35. Wells A, Grahovac J, Wheeler S, Ma B and Lauffenburger D: Targeting tumor cell motility as a strategy against invasion and metastasis. *Trends Pharmacol Sci* 34: 283-289, 2013.
36. Recher C, Ysebaert L, Beyne-Rauzy O, Mansat-De Mas V, Ruidavets JB, Cariven P, Demur C, Payrastra B, Laurent G, *et al*: Expression of focal adhesion kinase in acute myeloid leukemia is associated with enhanced blast migration, increased cellularity, and poor prognosis. *Cancer Res* 64: 3191-3197, 2004.
37. Hu C, Chen X, Wen J, Gong L, Liu Z, Wang J, Liang J, Hu F, Zhou Q, Wei L, *et al*: Antitumor effect of focal adhesion kinase inhibitor PF562271 against human osteosarcoma in vitro and in vivo. *Cancer Sci* 108: 1347-1356, 2017.
38. Jiang WG, Ye L, Ji K, Ruge F, Wu Y, Gao Y, Ji J and Mason MD: Antitumor effects of Yangzheng Xiaoji in human osteosarcoma: The pivotal role of focal adhesion kinase signalling. *Oncol Rep* 30: 1405-1413, 2013.



This work is licensed under a Creative Commons Attribution-NonCommercial-NoDerivatives 4.0 International (CC BY-NC-ND 4.0) License.